

HETE-2 LOCALIZATION AND OBSERVATIONS OF THE SHORT, HARD GAMMA-RAY BURST GRB020531

D. Q. LAMB,¹ G. R. RICKER,² J.-L. ATTEIA,³ K. HURLEY,⁴ N. KAWAI,^{5,6} Y. SHIRASAKI,^{5,9} T. SAKAMOTO,^{5,6,10} T. TAMAGAWA,⁶ C. GRAZIANI,¹ J.-F. OLIVE,³ A. YOSHIDA,^{5,7} M. MATSUOKA,⁸ K. TORII,⁶ E. E. FENIMORE,¹⁰ M. GALASSI,¹⁰ T. TAVENNER,¹⁰ T. Q. DONAGHY,¹ M. BOER,³ J.-P. DEZALAY,³ R. VANDERSPEK,² G. CREW,² J. DOTY,² G. MONNELLY,² J. VILLASENOR,² N. BUTLER,² J. G. JERNIGAN,⁴ A. LEVINE,² F. MARTEL,² E. MORGAN,² G. PRIGOZHIN,² S. E. WOOSLEY,¹¹ T. CLINE,¹² I. MITROFANOV,¹³ D. ANFIMOV,¹³ A. KOZYREV,¹³ M. LITVAK,¹³ A. SANIN,¹³ W. BOYNTON,¹⁴ C. FELLOWS,¹⁴ K. HARSHMAN,¹⁴ C. SHINOHARA,¹⁴ R. STARR,¹² J. BRAGA,¹⁵ R. MANCHANDA,¹⁶ G. PIZZICHINI,¹⁷ K. TAKAGISHI,¹⁸ AND M. YAMAUCHI¹⁸

Draft version November 20, 2018

ABSTRACT

The *HETE-2* (hereafter *HETE*) French Gamma Telescope (FREGATE) and the Wide-field X-ray Monitor (WXM) instruments detected a short ($t_{50} = 360$ msec in the FREGATE 85-300 keV energy band), hard gamma-ray burst (GRB) that occurred at 1578.72 SOD (00:26:18.72 UT) on 31 May 2002. The WXM flight localization software produced a valid location in spacecraft (relative) coordinates. However, since no on-board real-time star camera aspect was available, an absolute localization could not be disseminated. A preliminary localization was reported as a GCN Position Notice at 01:54:22 UT, 88 min after the burst. Further ground analysis produced a refined localization, which can be expressed as a 90% confidence rectangle that is 67 arcminutes in RA and 43 arcminutes in Dec (90% confidence region), centered at RA = +15^h 14^m 45^s, Dec = -19° 21'35''(J2000). An IPN localization of the burst was disseminated 18 hours after the GRB (Hurley et al. 2002b). A refined IPN localization was disseminated ≈ 5 days after the burst. This hexagonal-shaped localization error region is centered on RA = 15^h 15^m 03.57^s, -19° 24'51.00''(J2000), and has an area of ≈ 22 square arcminutes (99.7% confidence region). The prompt localization of this short, hard GRB by *HETE* and the anti-Sun pointing of the *HETE* instruments, coupled with the refinement of the localization by the IPN, has made possible rapid follow-up observations of the burst at radio, optical, and X-ray wavelengths. The time history of GRB020531 at high (> 30 keV) energies consists of a short, intense spike followed by a much less intense secondary peak. Its time history is thus similar to that seen in many short, hard bursts. Analysis of the FREGATE and WXM time histories gives durations for the burst of $t_{50} = 1.36$ s in the WXM 2 - 25 keV energy range, and 1.10 s, 0.86 s, 0.62 s, and 0.36 s in the FREGATE 6-13, 14-30, 31-84, and 85-400 keV energy bands. The duration of the burst thus increases with decreasing energy, which is similar to the behavior of long GRBs. The photon number flux, photon energy flux, and energy fluence of the burst in the 50-300 keV energy band in 1.25 seconds are 3.0 ph cm⁻² s⁻¹, 6.4×10^{-7} erg cm⁻² s⁻¹, and 8.0×10^{-7} erg cm⁻², respectively. The spectrum of the burst evolves from hard to soft, which is also similar to long GRBs. These similarities to the properties of long GRBs, and other similarities previously known, suggest that short, hard GRBs are closely related to long GRBs.

Subject headings: gamma rays: bursts (GRB020531)

¹ Department of Astronomy and Astrophysics, University of Chicago, 5640 South Ellis Avenue, Chicago, IL 60637.

² Center for Space Research, Massachusetts Institute of Technology, 70 Vassar Street, Cambridge, MA, 02139.

³ Centre d'Etude Spatiale des Rayonnements, CNRS/UPS, B.P.4346, 31028 Toulouse Cedex 4, France.

⁴ Space Sciences Laboratory, University of California at Berkeley, 601 Campbell Hall, Berkeley, CA, 94720.

⁵ Department of Physics, Tokyo Institute of Technology, 2-12-1 Ookayama, Meguro-ku, Tokyo 152-8551, Japan.

⁶ RIKEN (Institute of Physical and Chemical Research), 2-1 Hirosawa, Wako, Saitama 351-0198, Japan.

⁷ Department of Physics, Aoyama Gakuin University, Chitosedai 6-16-1 Setagaya-ku, Tokyo 157-8572, Japan.

⁸ Tsukuba Space Center, National Space Development Agency of Japan, Tsukuba, Ibaraki, 305-8505, Japan.

⁹ National Astronomical Observatory, Osawa 2-21-1, Mitaka, Tokyo 181-8588 Japan.

¹⁰ Los Alamos National Laboratory, P.O. Box 1663, Los Alamos, NM, 87545.

¹¹ Department of Astronomy and Astrophysics, University of California at Santa Cruz, 477 Clark Kerr Hall, Santa Cruz, CA 95064.

¹² NASA Goddard Space Flight Center, Greenbelt, MD, 20771.

¹³ Space Research Institute, Profsojuznaya Str. 84/32, 117810, Moscow, Russia.

¹⁴ Department of Planetary Sciences, Lunar and Planetary Laboratory, Tucson, AZ 85721-0092.

¹⁵ Instituto Nacional de Pesquisas Espaciais, Avenida Dos Astronautas 1758, São José dos Campos 12227-010, Brazil.

¹⁶ Department of Astronomy and Astrophysics, Tata Institute of Fundamental Research, Homi Bhabha Road, Mumbai, 400 005, India.

¹⁷ Consiglio Nazionale delle Ricerche (IASF), via Piero Gobetti, 101-40129 Bologna, Italy.

¹⁸ Faculty of engineering, Miyazaki University, Gakuen Kibanadai Nishi, Miyazaki 889-2192, Japan.

1. INTRODUCTION

It has been known for nearly a decade that gamma-ray bursts (GRBs) appear to fall into two classes: short (≈ 0.2 sec), harder bursts, which comprise 20-25% of all bursts; and long (≈ 20 sec), softer bursts, which comprise 75-80% of the total (Hurley et al. 1992; Lamb, Graziani, and Smith 1993; Kouveliotou et al. 1993). Norris, Scargle & Bonnell (2000). The spectra of the two classes of bursts differ: the spectra of the bursts become softer as the bursts become longer (Dezalay et al. 1992; Kouveliotou et al. 1993; Dezalay et al. 1996). There is also evidence that the brightness distributions of the two classes of bursts differ (Graziani and Lamb 1994; Belli 1997; Tavani 1998); however, the difference in the brightness distributions can be explained by the difference in their durations, which causes the sampling distance for short bursts to be smaller than for the long bursts (Graziani and Lamb 1994). In addition the V/V_{\max} values (Schmidt 2001) and the angular distributions (Kouveliotou et al. 1993) of the two classes appear to be identical.

Thanks to the rapid dissemination of accurate GRB localizations by *BeppoSAX* (Costa et al. 1997), much has been learned in the past five years about GRBs. This has included the discoveries that GRBs have X-ray (Costa et al. 1997), optical (van Paradijs et al. 1997), and radio (Frail et al. 1997) afterglows. Redshifts and host galaxies are now known for more than two dozen GRBs (see, e.g., Lamb 2002). However, all of these discoveries relate to long GRBs.

In contrast, to date nothing is known about the distance to or the nature of the short GRBs, despite extensive efforts. The Burst and Transient Source Experiment (BATSE) on the *Compton Gamma-Ray Observatory* localized numerous short GRBs in near-real time. Although many had large error boxes, one (trigger 6788) was localized to an error circle of ~ 30 square degrees, which was searched for an optical counterpart within 12 s to a magnitude of 14.98 (Kehoe et al. 2001). The results were negative. The Third Interplanetary Network (IPN) derived localizations for four short GRBs (000607, 001025B, 001204, and 010119) with delays of 15–65 hours. But in three of these cases, the opportunity for follow-up observations was compromised either by the burst being close to the Sun (000607, 65°) or close to the Galactic plane (001025B, $b \approx 4^\circ$; 010119, $b \approx 5^\circ$). Only one burst (001204) was optimally placed on the sky for follow-up observations. However, in this case the delay (65 hours) in deriving a localization for the burst hampered follow-up efforts. Despite an accepted *BeppoSAX* ToO program, no X-ray follow-up observations were possible because of Sun-angle or other operational constraints, except in the case of 001204. However, the delay in deriving the localization of this burst made the success of any X-ray follow-up observation unlikely, and therefore none was carried out.

In this Letter we report the detection and prompt localization of a short, hard GRB by *HETE-2* (hereafter *HETE*) (Ricker et al. 2002a,b). On 31 May 2002 at 1578.73 SOD (05:15:50.56) UT on 31 May 2002 UT, the *HETE-2* French Gamma Telescope (FREGATE) instrument (Atteia et al. 2002) and the Wide-field X-ray Monitor (WXM) instrument (Kawai et al. 2002) detected a bright, short (duration ~ 300 msec in the FREGATE 30-400 keV energy band), hard GRB. The prompt localization of this short, hard GRB by *HETE* and the anti-Sun pointing of the *HETE* instruments has made possible rapid follow-up observations of it at radio, optical, and X-ray wavelengths. We also describe the properties of GRB020531 derived from observations of it using the FREGATE and WXM instruments on *HETE*,

which provided unprecedented spectral and temporal coverage of this short, hard GRB.

2. OBSERVATIONS

2.1. Localization

The *HETE* FREGATE and WXM instruments detected a short (duration ~ 300 msec in the FREGATE 30-400 keV energy band), hard gamma-ray burst (GRB) that occurred at 1578.72 SOD (00:26:18.72 UT) on 31 May 2002. The fluence of the burst was not large enough for it to be detected by the *HETE* Soft X-Ray camera (SXC) (Monnelly et al. 2002). The WXM flight localization software produced a valid location in spacecraft (relative) coordinates. However, since no on-board real-time star camera aspect was available, an absolute localization could not be disseminated. A preliminary ground-analysis localization was reported as a GCN Position Notice at 01:54:22 UT, 88 minutes after the burst. Further ground analysis produced a refined localization, which can be expressed as a 90% confidence rectangle that is 67 arcminutes in RA and 43 arcminutes in Dec, centered at RA = $+15^{\text{h}} 14^{\text{m}} 45^{\text{s}}$, Dec = $-19^\circ 21'35''$ (J2000) (see Figure 1). The refined localization was reported as a GCN Position Notice at 03:57:14 UT, 211 minutes after the burst.

By restricting the search to the crossing window defined by the *HETE* position, a weak GRB was identified in the *Ulysses* data. An initial IPN localization of the burst was derived by triangulation using *HETE* FREGATE, *Ulysses* GRB and *Mars Odyssey* HEND data, and a 46 square arcminute error box was disseminated 18 hours after the GRB (Hurley et al. 2002b). This localization was further refined approximately five days after the burst. The resulting hexagonal-shaped localization error region is centered on RA = $15^{\text{h}} 15^{\text{m}} 03.57^{\text{s}}$, $-19^\circ 24'51.00''$ (J2000), and has an area of ≈ 22 square arcminutes (99.7% confidence region) (see Figure 1) (Hurley et al. 2002c).

We have used the imaging capabilities of the WXM to greatly improve the S/N of GRB020531 as seen by the WXM. Using the WXM photon time- and energy-tagged data (TAG data), we selected only WXM photons (1) during the portion of the burst that maximized the S/N of the burst time history, using Spiffy Trigger (Graziani 2002); (2) on the seven wires illuminated by the GRB but not by the bright Galactic X-ray source Sco X-1, which was in the field-of-view (FOV) of the WXM at the time; (3) on those portions of these seven wires that were illuminated by the burst; and (4) the bins on those portions of the wires that were illuminated by the burst, using the refined IPN localization of the burst (Hurley et al. 2002b) and the mask pattern of the coded aperture of the WXM. These “cuts” on the photon TAG data increased the S/N of the burst in the WXM data by nearly a factor of two. While these “cuts” on the WXM photon TAG data do not allow an improved localization of the GRB by the WXM, their success provides independent evidence that the refined IPN error region for the burst is correct.

2.2. Temporal Properties

Figure 2 shows the time history of GRB020531 in the WXM 2-25 keV energy band and in various FREGATE energy bands. Table lists the t_{50} and t_{90} durations of the burst in the WXM 2-25 keV energy band and in various FREGATE energy bands.

Figure 3 shows the burst time history in the entire WXM 2-25 keV energy band, and in four other WXM energy bands, utilizing the four “cuts” on the WXM photon TAG data that increase

the S/N of the burst in the WXM data, and that are described in §2.1 section.

The t_{50} and t_{90} durations of GRB020531 in the 85–400 keV energy band were 0.36 s and 0.74 s; thus GRB020531 is a short, hard GRB. Like many short bursts (see, e.g., 010119; Hurley et al. 2002), the time history of GRB020531 consists of a short, intense spike followed by a less intense and softer secondary peak. At low energies, the burst consists of two peaks, each lasting < 1 sec and separated by about 2 seconds (see Figure 3). Thus, at low energies, the primary and secondary peaks are comparable in duration and in intensity.

Figure 4 shows the t_{50} and t_{90} durations of GRB020531 in various energy bands. The duration of the burst increases with decreasing energy. A χ^2 fit to the t_{50} values, assuming that all of the values have the same relative uncertainty, yields $\log t_{50} = 0.42 - 0.38 \log(E/1\text{keV})$; a similar fit to the t_{90} values yields $\log t_{90} = 1.42 - 0.62 \log(E/1\text{keV})$. This behavior is similar to that seen in long GRBs (Fenimore et al. 1994).

2.3. Spectrum

Table 3 gives the S/N of the detection of the burst, the peak photon flux, the peak energy flux, and the energy fluence of the burst in the WXM and in various FREGATE energy band.

Table 4 gives the best-fit parameters for the spectrum of GRB020531 in the WXM and in FREGATE. Figure 5 shows the expected and observed photon counts in FREGATE energy loss bins from 6–400 keV (upper panel) and the residuals (lower panel) for the best fit power-law spectrum given in Table 4. Figure 6 shows the corresponding photon counts in the WXM energy loss bins from 2–25 keV for the four wires in the X-detector and the two wires in the Y-detector (Kawai et al. 2002) used in the WXM spectral fit.

The spectra derived independently in the WXM and in FREGATE are consistent with one another. The results show that the observed spectrum of GRB020531 is fully consistent with a single power-law spectrum with slope $\alpha = -1.2 \pm 0.06$. The power-law spectrum of GRB020531 extends from 2–400 keV, and shows no evidence of a cutoff at high energies to the highest energies (≈ 400 keV) observed by FREGATE.

We have explored the spectral evolution of the burst in the WXM 2–25 keV energy band. Using Spiffy Trigger (Graziani 2002), we found two time intervals during the burst that maximized the S/N of the time history. These two time intervals start 0.00 sec and 1.12 sec after the trigger time for the burst, and last $\Delta t_1 = 0.80$ sec and $\Delta t_2 = 0.72$ sec. We have used the four “cuts” on the WXM photon TAG data that are described in §2.1, and that increase the S/N of the burst in the WXM data, in order to determine the spectrum of the burst in the WXM 2–25 keV energy band in these two time intervals. Table 4 shows the resulting best-fit power-law parameters for these two time intervals. Comparing the value of the power-law index ($\alpha = 1.26 \pm 0.06$) for the spectrum during the first peak, as determined from the FREGATE data, and the value of the power-law index ($\alpha = 2.186_{-0.95}^{+1.38}$) for the spectrum during the second peak, as determined from the WXM data, provides evidence at the $\approx 90\%$ confidence level that the spectrum of the secondary peak is softer than the spectrum of the primary peak. Such spectral softening is similar to that seen in long GRBs (see, e.g., Band et al. 1993).

3. DISCUSSION

HETE has detected and localized GRB020531, a short, hard

burst. The prompt localization of the burst by *HETE* and the anti-Sun pointing of the *HETE* instruments, coupled with the later precise localization of the burst by the IPN, has allowed rapid follow-up of the GRB not only by small aperture, large FOV robotic telescopes (e.g., Park et al. 2002, Boer et al. 2002) but also by large aperture, modest FOV telescopes (e.g., Fox et al. 2002, Lamb et al. 2002, West et al. 2002, Miceli et al. 2002, Dullighan et al. 2002). Figure 7 shows that these observations have placed much more severe upper limits on any optical afterglow of a short, hard GRB than ever before. However, these constraints do not rule out the existence of optical afterglows of short, hard GRBs that are similar to the optical afterglows of long GRBs (see Hurley et al. 2002, Figure 3).

The time history of GRB020531 at high (> 30 keV) energies consists of a short, intense spike followed by a much less intense secondary peak. Its time history is thus similar to that seen in many short, hard bursts. The time history of GRB020531 at low (< 25 keV) energies consists of two peaks of similar duration (≈ 0.80 sec) and intensity, the first of which corresponds in time to the short, intense spike seen at high energies.

The spectrum of the short, intense spike is well described by a single power-law spectrum with index $\alpha = -1.2 \pm 0.06$ from 6–400 keV. Such a steep spectrum is quite unusual (Paciesas et al. 2001) but not unprecedented (see, e.g., Hurley et al. 2002; Figure 2 [GRB001204]) for short, hard GRBs. The steepness of the spectrum of GRB020531 may explain in part the fact that the WXM on *HETE* was able to detect and localize this particular short, hard burst, whereas the Wide-Field Cameras on *BeppoSAX* were ultimately unsuccessful in detecting or localizing any short, hard GRBs, despite great efforts (Gandolfi et al. 2002).

The spectrum of the secondary peak, which is comparable in duration and in intensity in the 2–25 keV energy band to the primary peak, is also well described by a single power-law spectrum, but the spectrum is softer than the spectrum of the primary peak at the 90% confidence level.

Two qualitatively different models have been suggested to explain GRBs: merging compact objects and the collapse of rotating massive stars. It is difficult to make short bursts in the collapsar model (MacFadyen & Woosley 1999) and there have been suggestions (e.g., Fryer, Woosley, & Hartmann 1999) that short hard bursts are the observational counterpart of merging neutron-star and neutron-star black-hole pairs. While collapsars and merging compact objects both get their energy from a hyperaccreting black hole, the dimension and mass of the disk is smaller in the latter, hence the time scale is shorter. If these mergers go on far from the galaxies where the compact objects are made, their afterglows might be faint.

The spectral and temporal behavior measured by *HETE* for GRB020531 could indicate a central engine that remains on with a declining power after the principal burst (reflecting a declining accretion rate?) or may be a consequence of the competition between internal and external shocks in making the GRB. The short time scale is certainly more consistent with the merging compact object hypothesis, but also possibly consistent with the supranova model (Vietri & Stella 1998, 1999) since the latter produces a similar compact disk and black hole. This could give a short burst should such bursts prove to be associated with massive stars.

The properties of GRB020531 as measured by *HETE* have different characteristics at different energies: more complex time structure at lower energies, increasing duration with de-

creasing energy, a power-law spectrum over the 2-400 keV energy range but spectral softening with time). These properties of GRB020531 as measured by *HETE* are similar to those of long bursts, and when taken together with the previously known properties of short, hard GRBs described in the Introduction (similar brightness distributions, V/V_{\max} values, angular distributions) suggest that short, hard GRBs are closely related to long GRBs.

4. CONCLUSIONS

HETE has detected and localized a short, hard GRB, establishing its capability to do so – and demonstrating that the detection and localization of short, hard GRBs in the hard x-ray energy band is possible. This has important implications for Swift and for other future GRB missions.

The prompt, precise localization of GRB020531 by *HETE* and the IPN have allowed rapid follow-up observations, which have placed much more severe limits on the brightness of any radio and optical afterglows from short, hard GRBs.

The complement of soft x-ray, hard x-ray, and gamma-ray instruments (SXC, WXM, and FREGATE) on *HETE* provides unprecedented temporal and spectral coverage of short, hard GRBs. With the currently projected long orbital lifetime (> 10 yrs) and excellent health of the *HETE* spacecraft and instruments, the results described for GRB020531 in this Letter demonstrate that *HETE* can continue to provide an unprecedented opportunity to study short, hard GRBs, and possibly to determine the distance to and the nature of these bursts.

ACKNOWLEDGMENTS

The *HETE* mission is supported in the US by NASA contract NASW-4690; in Japan, in part by the Ministry of Education, Culture, Sports, Science, and Technology Grant-in-Aid 13440063; and in France, by CNES contract 793-01-8479. KH is grateful for *Ulysses* support under Contract JPL 958056, for *HETE* support under Contract MIT-SC-R-293291, and for *Mars Odyssey* support under the NASA LTSA program. G. Pizzichini acknowledges support by the Italian Space Agency.

REFERENCES

- Atteia, J.-L., et al. 2002, *In-flight Performance and First Results from the FREGATE Instrument on HETE*, in WH2001⁷.
- bibitem[Band1993] Band, D. et al. 1993, ApJ, 413, 281
- Belli, B. 1997, in Proc. 25th Int. Cosmic-Ray Conf. (Durban), 41
- Boer, M. Klotz, A., Atteia, J.-L., Pollas, C. & Pinna, H. 2002, GCN Circular 1408
- Butler, N., Dullighan, A., Ford, P., Monnelly, G., Ricker, G., Vanderspek, R., Hurley, K. & Lamb, D. 2002, GCN Circular 1415
- Costa, E. et al. 1997, IAU Circular No. 6576
- Dezalay, J.-P. et al. 1992, in AIP Conf. Proc. 265, Gamma-Ray Bursts, ed. W. Paciesas & G. Fishman (New York: AIP), 304
- Dezalay, J.-P. et al. 1996, ApJ, 471, L27
- Dulligan, Monnelly, G., Butler, N., Vanderspek, R., Ford, P. & Ricker, G. 2002, GCN Circular 1411
- bibitem[Fenimore1994] Fenimore, E. E. 1994, ApJ, 547, 315
- Fox, D. & Bloom, J. S. 2002, GCN Circular 1400
- Frail, D. et al. 1997, Nature 389, 261
- Frail, D. A. & Berger, e. 2002, GCN Circular 1418
- Fryer, C. L., Woosley, S. E., Hartmann, D. H. 1999, ApJ, 526, 152
- Gandolfi, G. et al. 2002, *BeppoSAX Results on Short Gamma-Ray Bursts*, in WH2001**.
- Graziani, C., Lamb, D. Q. 1994, in AIP Conf. Proc. 307, Gamma-Ray Bursts, ed. G. J. Fishman, J. J. Brainerd, and K. Hurley (New York: AIP), 227
- Hurley, K. 1992, in AIP Conf. Proc. 265, Gamma-Ray Bursts, ed. W. Paciesas & G. Fishman (New York: AIP), 3
- Hurley, K. 2002a, ApJ, 567, 447
- Hurley, K., et al. 2002b, GCN Circ. 1402
- Hurley, K., et al. 2002c, GCN Circ. 1407
- Kawai, N., et al. 2002, *In-Orbit Performance of the WXM Instrument on HETE*, in WH2001**.
- Kehoe, R. et al. 2001, ApJ, 554, L159
- Kouveliotou, C. et al. 1993, ApJ, 413, L101
- Lamb, D. Q. 2002, *Gamma-Ray Bursts as a Probe of Cosmology*, in WH2001**.
- Lamb, D. Q., Graziani, C. & Smith, I. A. 1993, ApJ, 413, L11
- Lamb, D. Q. et al. 2002, GCN Circular 1403
- MacFadyen, A. & Woosley, S. 1999, ApJ, 524, 262
- Miceli, A., Lamb, D. Q., Zucker, D., Covey, K., Dembicky, J. & Hastings, N. C. 2002, GCN Circular 1416
- Monnelly, G. et al. 2002, *HETE Soft X-Ray Camera Imaging: Calibration, Performance, and Sensitivity*, in WH2001**.
- Paciesas, W. S., Preece, R. D., Briggs, M. S., and Malozzi, R. S. 2001, in Gamma-Ray Bursts in the Afterglow Era, (Rome, Italy, 17-20 October 2000), ESO Astrophysics Symposia, Springer (Berlin), p. 13
- van Paradijs, J. et al. 1997, Nature 386, 686
- Park, H. S., Williams, G. G., Lindsay, K. 2002, GCN Circular 1404
- Ricker, G. R., et al. 2002, GCN Circ. 1399
- Ricker, G.R., et al. 2002, *High Energy Transient Explorer (HETE): Mission and Science Overview*, in WH2001**.
- Ruffert, M. & Janka, H. 1999, A&A, 344, 573
- Schmidt, M. 2001, ApJ, 559, L79
- Tavani, M. 1998, ApJ, 497, L21
- Vietri, M., & Stella, L. 1998, ApJL, 507, L45
- Vietri, M., & Stella, L. 1999, ApJL, 527, L43
- West, D. 2002, GCN Circular 1406

⁷ WH2001 = *Gamma-Ray Burst and Afterglow Astronomy 2001: A Workshop Celebrating the First Year of the HETE Mission*, Woods Hole, MA, November 2001, to be published in the AIP Conference Proceedings (AIP Press: New York).

TABLE 1
GRB020531 ERROR BOX COORDINATES

Source	$\alpha_{J2000.0}$	$\delta_{J2000.0}$	Comment
HETE WXM	15 14 45	-19 21 35	center
	15 17 00	-19 43 00	corner
	15 17 00	-19 00 00	corner
	15 12 30	-19 00 00	corner
	15 12 30	-19 43 00	corner
IPN	15 15 03.57	-19 24 51.00	center
	15 14 53.98	-19 24 18.15	corner
	15 15 14.46	-19 21 38.39	corner
	15 15 17.07	-19 21 35.32	corner
	15 15 12.51	-19 25 32.46	corner
	15 14 53.75	-19 27 58.57	corner
	15 14 49.67	-19 28 03.27	corner

Note. — Units of right ascension are hours, minutes, and seconds; units of declination are degrees, arcminutes, and arcseconds.

TABLE 2
TEMPORAL PROPERTIES OF GRB020531.

Instrument	Energy Band (keV)	t_{50} (s)	t_{90} (s)
HETE WXM	2 - 25	1.36	4.56
HETE FREGATE	6-13	1.10	5.58
	14-30	0.86	3.46
	31-84	0.62	4.52
	85-400	0.36	0.74

TABLE 3
ENERGY EMISSION PROPERTIES OF GRB020531.

Energy Band (keV)	Photon Flux ($\text{ph cm}^{-2} \text{s}^{-1}$)	Energy Flux ($\text{erg cm}^{-2} \text{s}^{-1}$)	Energy Fluence (erg cm^{-2})
2 - 25	2.9	$(2.7 \pm 0.8) \times 10^{-8}$	$(4.9^{+1.5}_{-1.4}) \times 10^{-8}$
8 - 400	8.4	10.1×10^{-6}	12.7×10^{-7}
32 - 400	4.4	9.1×10^{-7}	11.4×10^{-7}
25 - 100	3.0	2.6×10^{-7}	3.1×10^{-7}
50 - 300	3.0	6.4×10^{-7}	8.0×10^{-7}

Note. — All WXM parameters are for a joint fit to six wires (XA0, XA1, XA2, XB0, YB0, and YB1).

TABLE 4
PARAMETERS FOR BEST-FIT POWER-LAW SPECTRUM OF GRB020531.

Instrument	Δt (s)	Energy Band (keV)	Scale Factor	Power-Law Index α
WXM	0.00-1.84	2 - 25	$3.936^{+0.99}_{-0.93}$	$1.57^{+0.48}_{-0.44}$
	0.00-0.80	"	—	$1.15^{+0.80}_{-0.54}$
	1.12-1.84	"	—	$3.06^{+2.55}_{-1.27}$
FREGATE	(-0.145)-(+1.31)	6-400	$(8.05 \pm 0.56) \times 10^{-2}$	1.26 ± 0.06

Note. — The scale factor for the WXM fit is normalized at 1 keV, while that for the FREGATE fit is normalized at 30 keV. The WXM parameters are for a joint fit to six wires (XA0, XA1, XA2, XB0, YB0, and YB1).

GRB020531

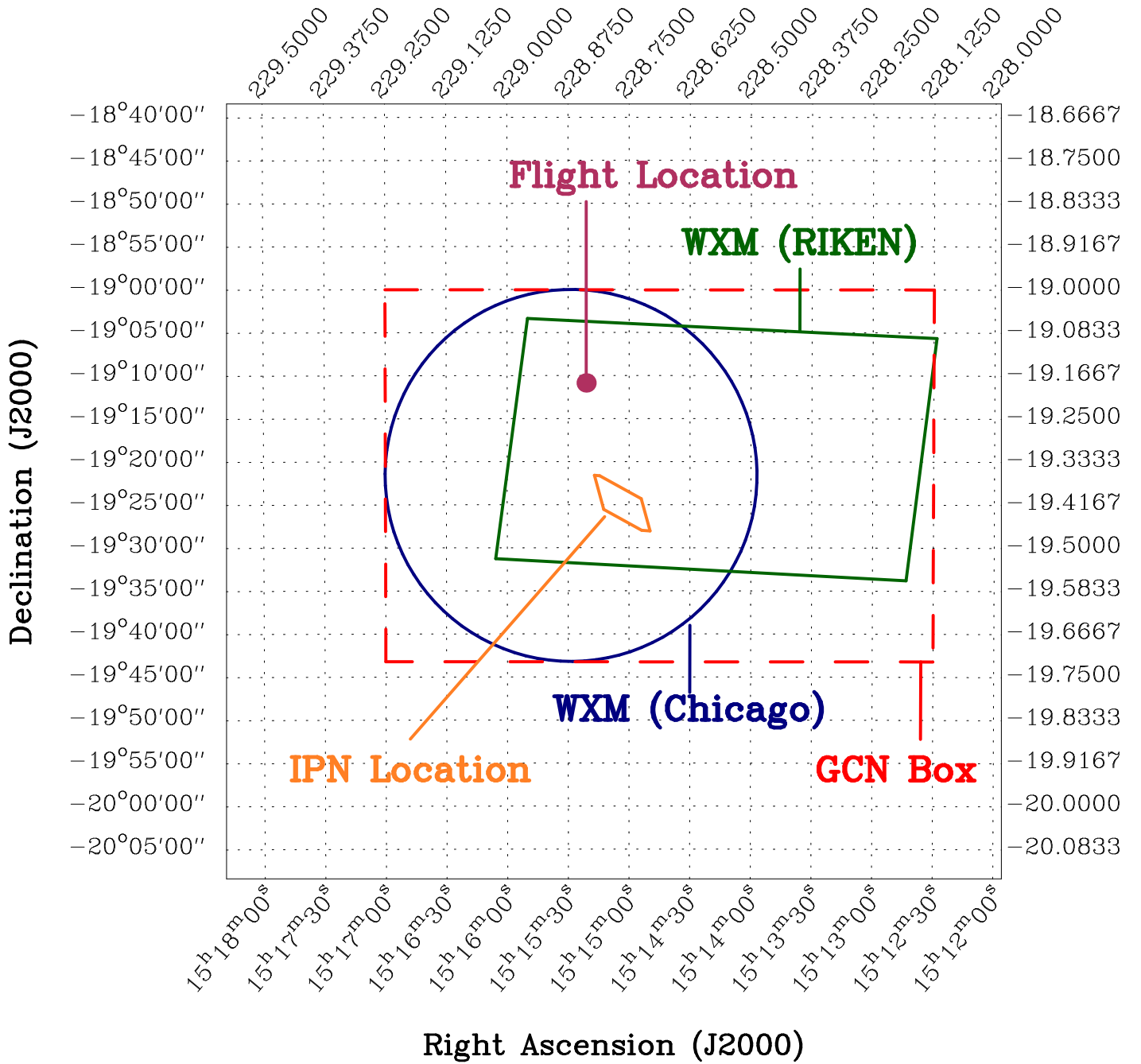


FIG. 1.— The final rectangular HETE WXM error box for GRB020531 (dashed line). The rectangle completely encloses the Chicago 90% confidence region error circle and RIKEN 90% confidence region error rectangle (which utilized the same data). Note that the WXM flight location lies well inside the confidence region. Also shown is the hexagonal-shaped refined IPN error box for GRB020531 (thin solid line), determined by triangulation using the *HETE* FREGATE, *Ulysses* GRB, and *Mars Odyssey* HEND data for the burst.

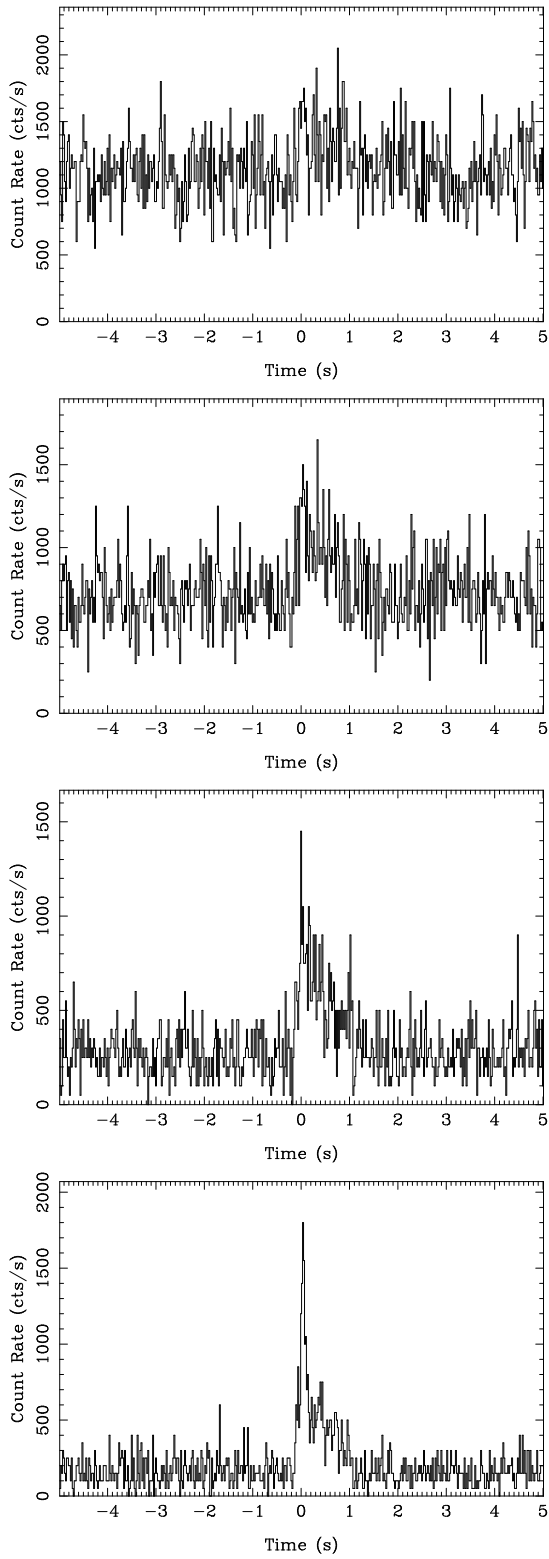


FIG. 2.— FREGATE time histories of GRB020531, binned in 80 msec bins. Top to bottom: the 6-13 keV, 13-30 keV, 30-85 keV, and 85-300 keV bands.

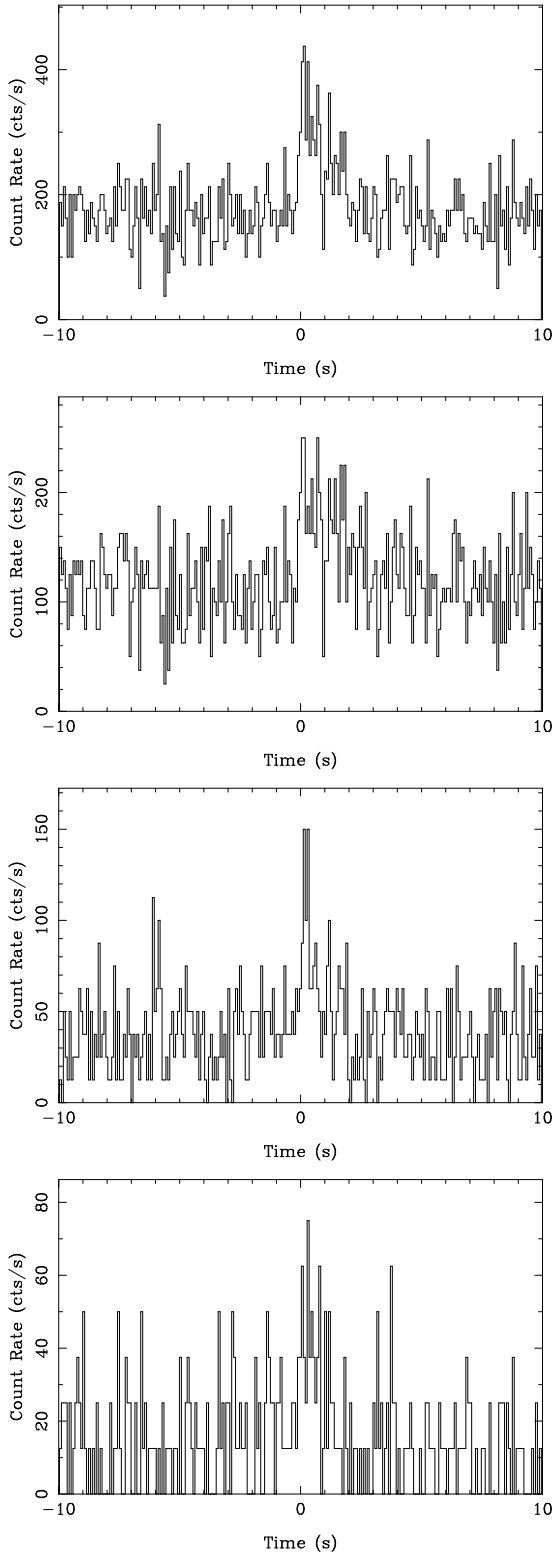


FIG. 3.— Time history of GRB020531 in the WXM 2-25 keV, 2-8 keV, 8-15 keV, and 15-25 keV energy bands, binned in 80 msec bins.

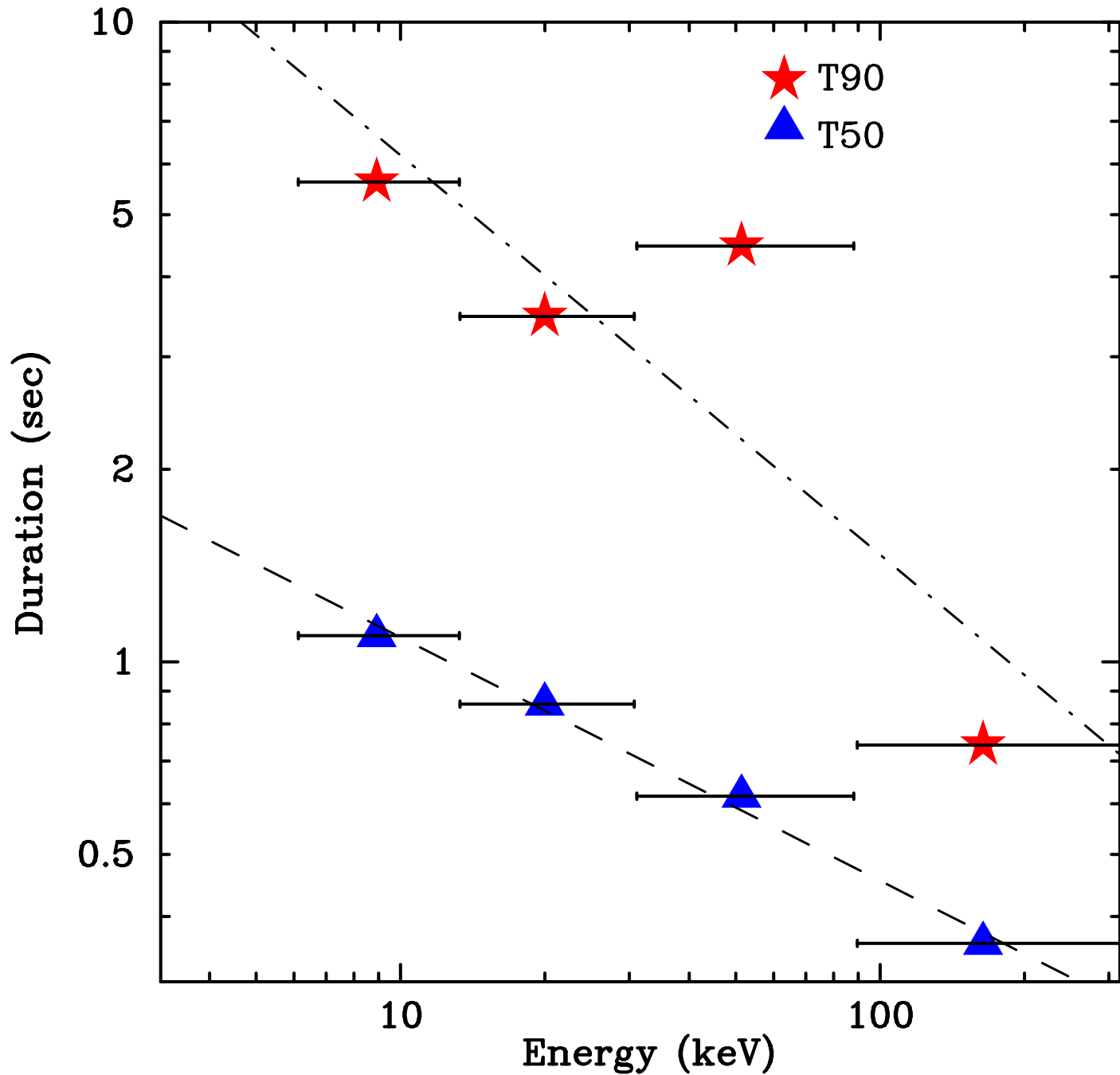


FIG. 4.— Duration of GRB020531 versus energy. The energy bins have been chosen so that each contains approximately the same number of photons. The durations t_{50} and t_{90} increase with decreasing energy as $E^{-0.38}$ and $E^{-0.62}$, respectively. This behavior is similar to that seen in long GRBs.

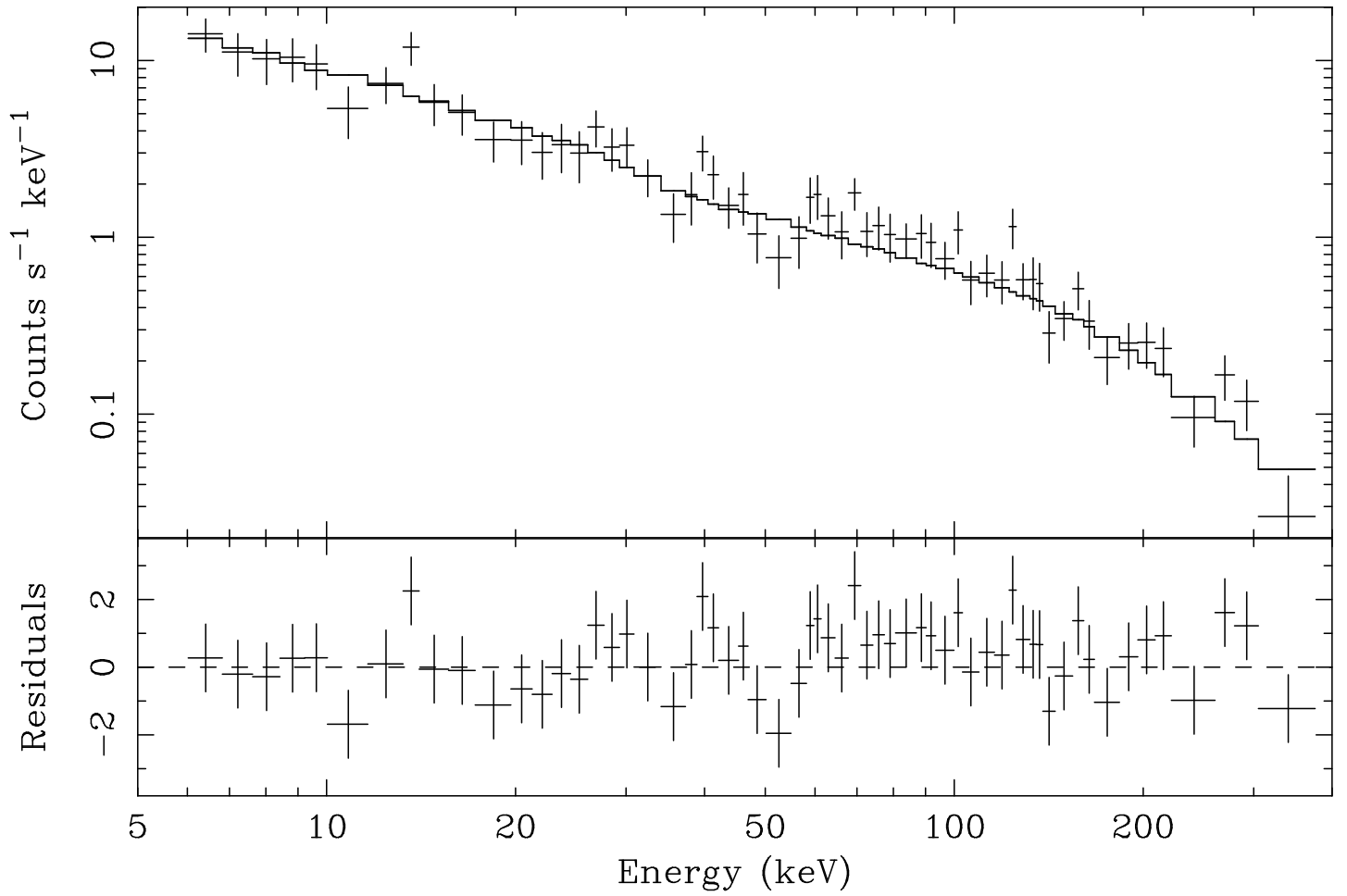


FIG. 5.— Upper panels: Observed counts (crosses) compared to predicted counts (histogram) for the best-fit spectrum in the FREGATE energy band 6-400 keV during the first 0.00-1.25 sec of the burst. Lower panels: residuals.

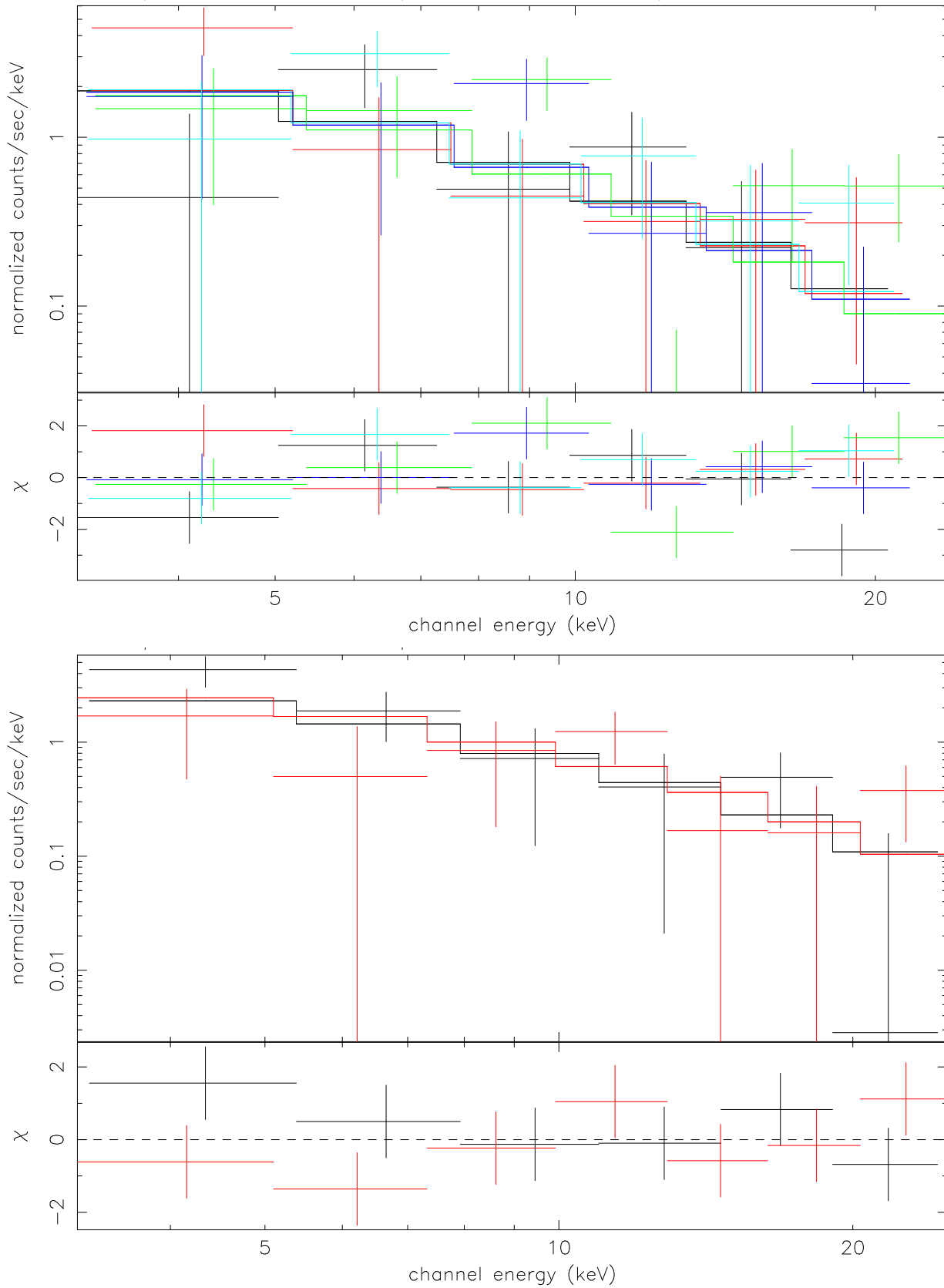


FIG. 6.— Observed counts compared to predicted counts for the best-fit spectrum in the WXM energy band 2-25 keV for the first 1.84 seconds of the burst, and the residuals. A specific detector response matrix is calculated for each anode wire. Top panels: Observed counts (crosses) compared to predicted counts (histograms) for wires XA0, XA1, XA2, and XB0 (upper panel); residuals (lower panel). Bottom panels: Observed counts (crosses) compared to predicted counts (histograms) for wires YB0, and YB1 (upper panel); residuals (lower panel).

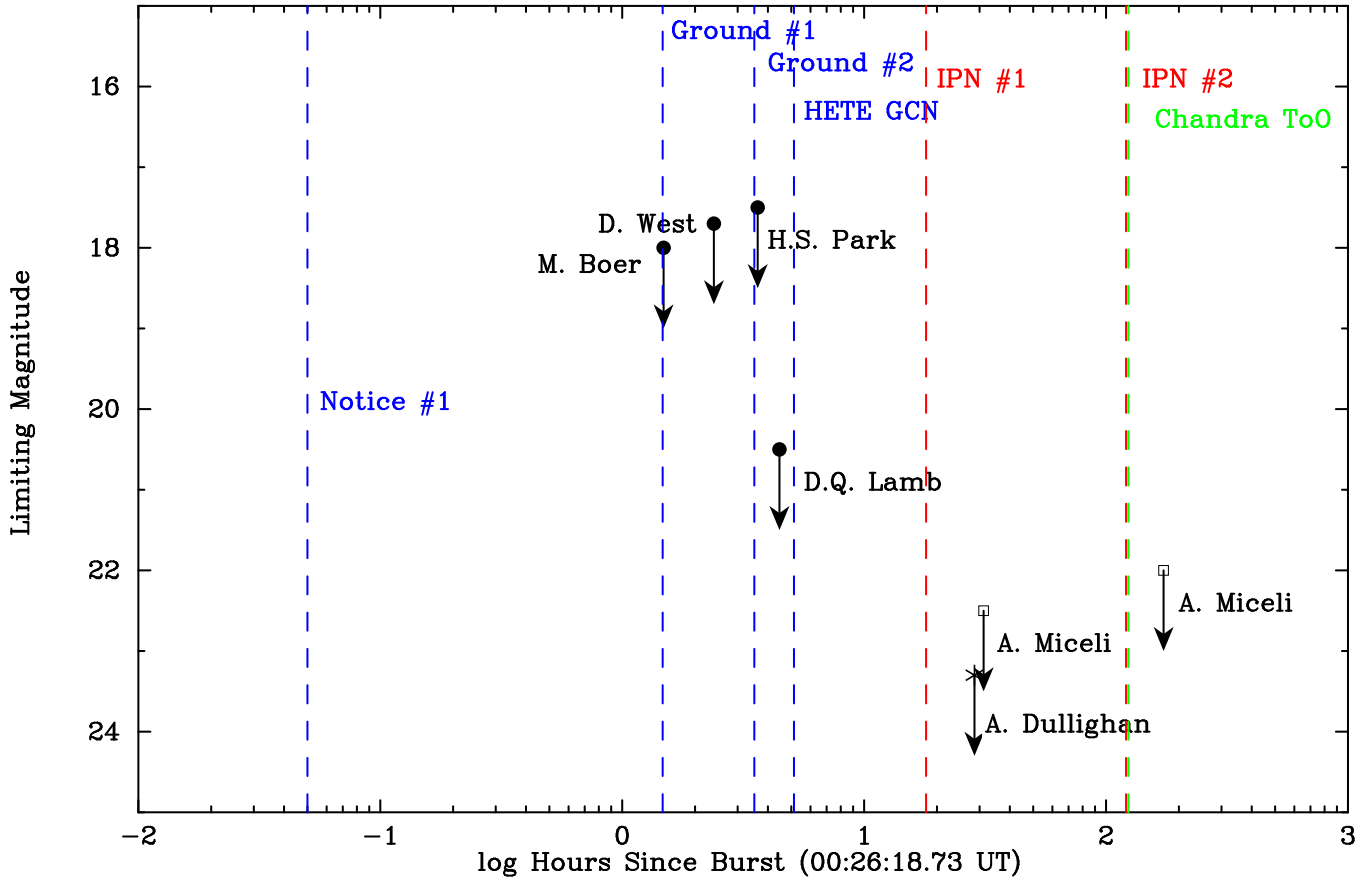


FIG. 7.— Limiting magnitudes versus time for any optical afterglow from follow-up observations of GRB020531. The limiting magnitudes shown include both limits derived using small aperture, large FOV robotic telescopes (Park et al. 2002, Boer et al. 2002, West), a small aperture, modest FOV telescope (West et al. 2002), and large aperture, small FOV telescopes (Lamb et al. 2002, West et al. 2002, Miceli et al. 2002, Dullighan et al. 2002).